High Power Distributed Balanced Photodetectors with High Linearity

M. Saif Islam, T. Jung, S. Mathai, T. Chau, A. Rollinger, T. Itoh, and Ming C. Wu
Deborah L. Sivco†, and Alfred Y. Cho†

ABSTRACT

A distributed *balanced* photodetector with high saturation photocurrent has been experimentally demonstrated. The maximum linear DC photo-current of 33 mA/branch is equivalent to 66mA in single-ended photodetectors. The AC linearity at high photocurrents is also investigated.

I. INTRODUCTION

Balanced receivers are very attractive for high performance microwave photonic links. They can suppress the laser relative intensity noise (RIN) and the amplified spontaneous emission noise (ASE) from erbium doped fiber amplifiers (EDFA) [1,2]. This enables the link to achieve shot noise-limited performance at high optical powers. The link gain, spurious-free dynamic range (SFDR), and the noise figure are greatly improved.

To realize these advantages, balanced photodetectors with high saturation photocurrents and broad bandwidth are needed. Previously, we reported a novel monolithic distributed balanced photodetector [3]. Broadband (1 to 12 GHz) noise suppression was demonstrated [4]. Maximum noise suppression of 24 dB was observed at the relaxation oscillation frequency of the laser [4]. However, the maximum DC photocurrent was limited to 12 mA, and the linearity of the balanced photodetectors under high power operation was not investigated.

The authors are with the Department of Electrical Engineering, 63-128 Eng IV, University of California, Los Angeles, CA 90095, USA. Tel: (310) 794-9309, Fax: (310) 794-5513. e-mail: wu@ee.ucla.edu
†D.L. Sivco and A.Y. Cho are with Lucent Technologies, Bell Laboratories, Murray Hill, NJ 07974, USA.

In this paper, we report on an improved distributed balanced photodetector that has a maximum linear DC photocurrent of 33 mA (equivalent to 66 mA from regular, non-balanced photodetectors). We have also investigated the AC linearity of devices under high power operations.

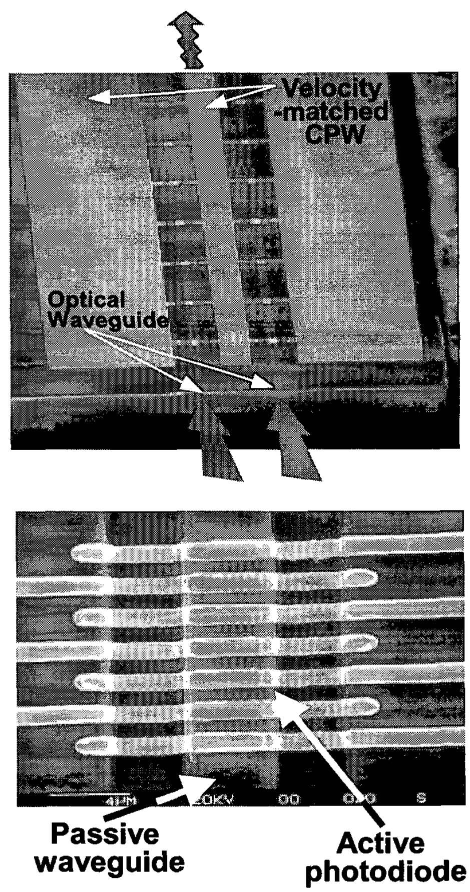

Fig. 1. (Top) SEM micrograph of the distributed balanced receiver. MSM photodiodes are distributed along the optical waveguide. (Bottom) Close-up view of a MSM photodiode on top of a multimode waveguide.

II. DESIGN AND FABRICATION

Figure 1 shows the scanning electron micrograph (SEM) of the distributed balanced photodetector. It consists of two input optical waveguides, two arrays of high-speed metal-semiconductor-metal (MSM) photodiodes distributed along two passive optical waveguides, and a 50Ω coplanar waveguide (CPW) microwave transmission line. The detector operates in balanced mode when a voltage bias is applied between the two ground electrodes of the CPW. The photodiode arrays provide periodic capacitance loading to slow down the microwave velocity. By adjusting the length and separation of the photodiodes, velocity matching between the CPW and the optical waveguides is achieved. The photodiodes are designed to operate below saturation under high optical input by coupling only a small fraction of light from the passive waveguide to each individual photodiode.

The primary improvements we have made in this device are (1) continuous waveguide transitions between passive guide and active photodiodes, and (2) multimode optical waveguides. In our previous devices [3,4], the optical waves were weakly confined by ridge structures, and the discontinuity of the waveguide width also resulted in excessive optical loss at the waveguide transitions. Here, we employ a strong index-guided optical waveguide with uniform width for both the active photodiode and the passive waveguide. Particular care has been taken to ensure the continuity of the MSM fingers across the 1.5-μm-high waveguide, as shown in Fig. 1(b).

We have also employed a 5-μm-wide multimode waveguide to increase the saturation optical power. Multimode waveguide has been employed in lumped waveguide photodetectors to improve fiber coupling efficiency [5]. Here, we observed almost three-fold improvement in the maximum photocurrent level of the multimode waveguide distributed photodetectors with respect to single mode waveguide devices in our first demonstration. This is an indication of better guiding and uniform distribution of input power to multiple photodiodes in the receiver. Beam propagation method (BPM) was used to simulate and optimize the waveguide performance. Since the microwave velocity can only be matched to the group velocity of one optical mode, there is some inherent velocity mismatch in multimode devices. However, the mismatch is small (< 10%) and the bandwidth limit due to velocity mismatch is greater than 150 GHz, which is much higher than the transit time-limited bandwidth of our current device.

III. MEASUREMENTS AND RESULTS

The balanced receiver exhibits very good electrical and optical characteristics. The dark current is measured to be <0.2 nA/diode at 10 V bias. The DC response is found to be flat above 4V bias. The responsivity is 0.28A/W at 4V bias (without AR coating). Figure 2 shows measured photocurrent in one branch of the photodetector versus the input optical power. The photocurrent remains linear up to 33 mA. The device fails at higher photocurrent due to thermal runaway. It should be noted that the

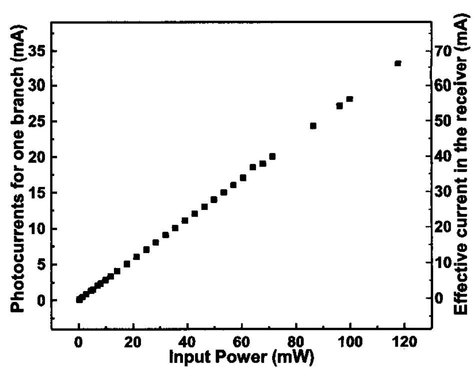

Fig. 2. DC photocurrent vs input optical power. The DC photocurrent remains linear up to 33mA.

33mA photocurrent in balanced photodetector is equivalent to 66 mA photocurrent in single-ended photodetectors because the RF signals from both branches of photodiodes add in phase.

In most previous works, nonlinear distortions are observed in photodetectors with photocurrents greater than a couple of mA's. Nonlinear distortions were attributed to high density of photogenerated carriers at high optical power, which result in nonlinear carrier velocity [6]. Distortion was also observed at low optical power due to a change in photodetector impedance [7].

Two-tone modulation was employed to investigate the nonlinear distortions of the distributed photodetector. To avoid the distortion of the modulator, optical heterodyning of three external-cavity tunable lasers were employed to generate two RF tones at 13 and 14.5 GHz on one branch of the balanced receiver. The output of the receiver was directly connected to a microwave spectrum analyzer. We did not observe any 2nd or 3rd order harmonics (H2 or H3) or 3rd order intermodulation distortion with photocurrent as high as 20 mA. This demonstrates the high AC linearity of the receiver.

The frequency response of a single branch of the photodetector was measured under various optical input powers. The bandwidth of the photodetector remained unchanged (14.5 GHz) when the photocurrent is varied from 0.5 mA to 14.5 mA. Figure 3 shows the AC response of the phodetector at RF frequencies of 10 and 15 GHz versus the photocurrent. The AC response is proportional to the square of the photocurrent up to the highest photocurrent measured (14.5 mA, limited by the setup). This confirmed the linearity of the photodetector.

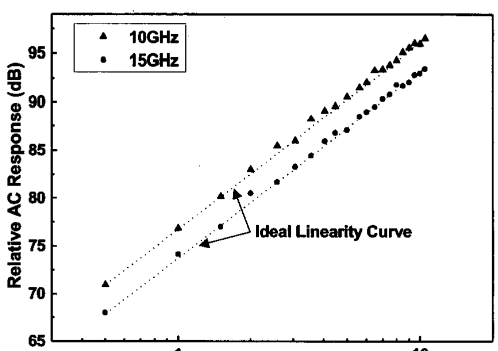

Fig. 3. Measured AC linearity of the balanced receiver at different photocurrents. The dotted line shows the ideal linearity curves.

To investigate the AC linearity of the receiver in balanced mode, we designed a setup as depicted in Figure 4. An external cavity tunable laser with 1550-nm wavelength and 3 dBm output power is employed as the optical source. It is amplified by an EDFA and then filtered by an optical bandpass filter with 2-nm bandwidth. The microwave signal

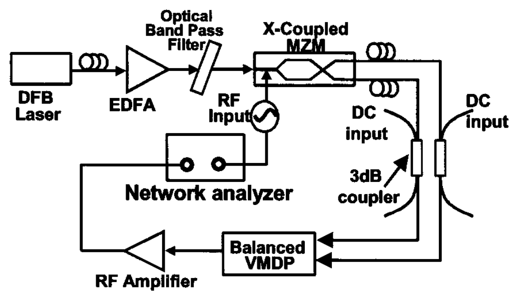

Fig. 4. Setup for measuring the nonlinearity of the distributed balanced receiver.

was modulated onto the optical carrier by an X-coupled Mach-Zehnder modulator (MZM), which produces two complimentary outputs. The outputs are coupled to the balanced receiver by two lensed fibers. Another external cavity laser is employed to provide additional DC input. It is similarly amplified

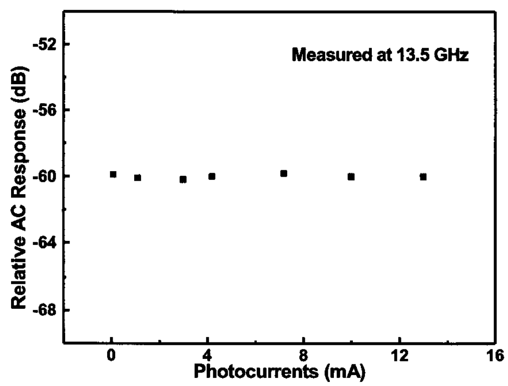

Fig. 5. Measured AC response of the balanced receiver at different photocurrent level. The response is linear at the photocurrent range within the experimental error of 0.5 dB.

by another EDFA, split into two equal branches and then combined with the AC signals through two 3dB couplers. The wavelengths of the external cavity lasers are separated far enough to avoid interference of their beating frequency. The polarization orientations of both AC and both DC signals are independently optimized by four polarization controllers. The AC photocurrents were set to 160 μA for each branch of the receiver and the DC currents were allowed to vary from 1 mA to 13 mA (limited by our setup). Figure 5 shows the AC output power versus the DC photocurrent at a frequency of 13.5 GHz. In this photocurrent range, the AC signal remained equal in magnitude within an experimental error of half a dB. To our knowledge, this is the first report of the AC linearity measurement of balanced receivers.

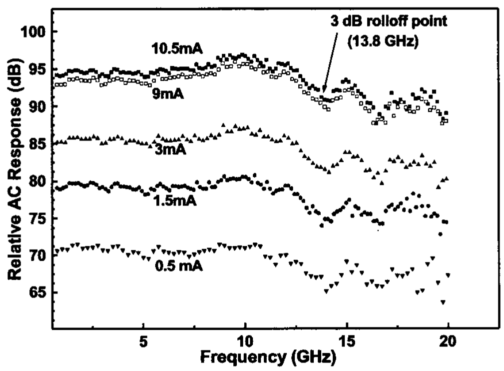

Fig. 6. Measured frequency response of the distributed balanced receiver at various DC photocurrents.

For optimum RF link performance, high power receivers must maintain their high-speed performance at high DC photocurrents. Most photodiodes suffer from degradation in the frequency response at high photocurrents due to the electric field screening effect [6,7]. Using the setup shown in Figure 4, we measured the AC response of the balanced receiver at various photocurrent levels. No DC input was used in this measurement. Figure 6 shows the relative AC responsivity of the balanced receiver with photocurrents varying from 0.5 mA to 10.5 mA. The frequency response at 10.5 mA is identical to that at 0.5 mA, indicating excellent linearity of the balanced receiver at high photocurrent. The 3-dB bandwidth of the balanced receiver (13.8 GHz) is slightly lower than that of the individual branches (14.5 GHz). This may be due to parasitics of the biasing capacitor (120 pF) on one ground of the probe for DC biasing and RF signal collection.

IV. CONCLUSION

We have successfully demonstrated a distributed balanced photodetector with high photocurrent and excellent linearity. It has a maximum linear DC photocurrent of 33 mA (equivalent to 66 mA in single-ended photodetectors). The device also exhibited excellent AC linearity at high photocurrents. The experimental results indicate that the distributed balanced photodetector will have a major impact on high performance RF photonic systems.

V. ACKNOWLEDGEMENT

The authors would like to acknowledge Dr. D. T.K. Tong of Lucent Technologies-Bell Lab., Homedel NJ, USA, for his helpful suggestions about the experimental setup. This project was supported by ONR MURI on RF photonics, NRAO and UC MICRO.

REFERENCE:

[1] C. H. Cox, III, G. E. Betts, and L. M. Johnson, "An analytic and experimental comparison of direct and external modulation in analog fiber-optic links," *IEEE Transaction on Microwave Theory and Techniques*, vol. 38, no. 5, pp 501-509, May 1991.

[2] L T. Nichols, K. J. Williams and R. D. Esman, "Optimizing the ultrawideband photonic link," *IEEE Transaction on Microwave Theory and Techniques*, vol. 45, no. 8, pp. 1384 - 1389, 1997.

[3] M. S. Islam, T. Chau, A. Nespola, S. Mathai, A. R. Rollinger, W. R. Deal, T. Itoh, M. C. Wu, D. L. Sivco and A. Y. Cho "Distributed balanced photodetectors for high performance RF photonic links," *IEEE Photon. Technol. Lett.*, vol. 11, no 4 pp. 457-560, April 1999.

[4] M. S. Islam, T. Chau, S. Mathai, T. Itoh, M. C. Wu, D. L. Sivco, and A.Y. Cho, "Distributed balanced photodetectors for broadband noise suppression," *IEEE Transaction on Microwave Theory and Techniques,* vol. 47, no. 7, pp. 1282-1288, *1999.*

[5] K. Kato, S. Hata, K. Kawano, J. Yoshida, and A. Kozen, "A high efficiency 50 GHz InGaAs multimode waveguide photodetector," *IEEE J. Quantum Electron.*, vol. 28, pp.2728-2735, 1992.

[6] K. J. Williams, R. D. Esman, and M. Dagenais, "*Nonlinearities in p-i-n microwave photodetectors*," J. Lightwave Technol., vol. 14, pp. 84-96, 1996.

[7] Jian, H., Yu, P. K. L., "*Equivalent circuit analysis of harmonic distortions in photodiode*," *IEEE Photon. Technol. Lett.*, vol. 10, no. 11, pp. 1608-1611, 1998.